NATO Science for Peace and Security Series - C:
Environmental Security

Nanotechnology in the Security Systems

Edited by
Janez Bonča
Sergei Kruchinin

Springer

NATO
OTAN
This publication is supported by: The NATO Science for Peace and Security Programme

NATO Science for Peace and Security Series

This Series presents the results of scientific meetings supported under the NATO Programme: Science for Peace and Security (SPS).

The NATO SPS Programme supports meetings in the following Key Priority areas: (1) Defence Against Terrorism; (2) Countering other Threats to Security and (3) NATO, Partner and Mediterranean Dialogue Country Priorities. The types of meeting supported are generally "Advanced Study Institutes" and "Advanced Research Workshops". The NATO SPS Series collects together the results of these meetings. The meetings are co-organized by scientists from NATO countries and scientists from NATO's "Partner" or "Mediterranean Dialogue" countries. The observations and recommendations made at the meetings, as well as the contents of the volumes in the Series, reflect those of participants and contributors only; they should not necessarily be regarded as reflecting NATO views or policy.

Advanced Study Institutes (ASI) are high-level tutorial courses to convey the latest developments in a subject to an advanced-level audience

Advanced Research Workshops (ARW) are expert meetings where an intense but informal exchange of views at the frontiers of a subject aims at identifying directions for future action

Following a transformation of the programme in 2006 the Series has been re-named and re-organised. Recent volumes on topics not related to security, which result from meetings supported under the programme earlier, may be found in the NATO Science Series.

The Series is published by IOS Press, Amsterdam, and Springer, Dordrecht, in conjunction with the NATO Emerging Security Challenges Division.

Sub-Series

A.	Chemistry and Biology	Springer
B.	Physics and Biophysics	Springer
C.	Environmental Security	Springer
D.	Information and Communication Security	IOS Press
E.	Human and Societal Dynamics	IOS Press

http://www.nato.int/science
http://www.springer.com
http://www.iospress.nl

Series C: Environmental Security

Nanotechr
Systems

edited by

Janez Bonča

Faculty of Mathematics a
Department of Theoretic
University of Ljubljana
J. Stefan Institute
Ljubljana, Slovenia

and

Sergei Kruchi

Bogolyubov Institute for
Kiev, Ukraine

Springer
Published in Cooperatio

Nanotechnology in the Security Systems

edited by

Janez Bonča
Faculty of Mathematics and Physics
Department of Theoretical Physics
University of Ljubljana
J. Stefan Institute
Ljubljana, Slovenia

and

Sergei Kruchinin
Bogolyubov Institute for Theoretical Physics
Kiev, Ukraine

Springer
Published in Cooperation with NATO Emerging Security Challenges Division

Proceedings of the NATO Advanced Research Workshop on
Nanotechnology in the Security Systems
Yalta, Ukraine
29 September – 3 October 2013

Library of Congress Control Number: 2014945233

ISBN 978-94-017-9052-9 (PB)
ISBN 978-94-017-9004-8 (HB)
ISBN 978-94-017-9005-5 (e-book)
DOI 10.1007/978-94-017-9005-5

Published by Springer,
P.O. Box 17, 3300 AA Dordrecht, The Netherlands.

www.springer.com

Printed on acid-free paper

All Rights Reserved
© Springer Science+Business Media Dordrecht 2015
This work is subject to copyright. All rights are reserved by the Publisher, whether the whole or part of the material is concerned, specifically the rights of translation, reprinting, reuse of illustrations, recitation, broadcasting, reproduction on microfilms or in any other physical way, and transmission or information storage and retrieval, electronic adaptation, computer software, or by similar or dissimilar methodology now known or hereafter developed. Exempted from this legal reservation are brief excerpts in connection with reviews or scholarly analysis or material supplied specifically for the purpose of being entered and executed on a computer system, for exclusive use by the purchaser of the work. Duplication of this publication or parts thereof is permitted only under the provisions of the Copyright Law of the Publisher's location, in its current version, and permission for use must always be obtained from Springer. Permissions for use may be obtained through RightsLink at the Copyright Clearance Center. Violations are liable to prosecution under the respective Copyright Law.

The use of general descriptive names, registered names, trademarks, service marks, etc. in this publication does not imply, even in the absence of a specific statement, that such names are exempt from the relevant protective laws and regulations and therefore free for general use.

While the advice and information in this book are believed to be true and accurate at the date of publication, neither the authors nor the editors nor the publisher can accept any legal responsibility for any errors or omissions that may be made. The publisher makes no warranty, express or implied, with respect to the material contained herein.

Preface

These proceedings of the
held at the "Yalta" Hotel,
emerged as a result of n
participants.

Yalta workshop focuse
nanotechnology and securi

Recent advances in na
physical phenomena arise
comparable with the funda
rials. There have been ma
workshop and some entire
undertaken. The program
discussions on several eme
and sensors. Theoretical
technological achievement
in the field of nanotechn
nanocomposite multifuncti
nanoanalyzers. In the sessi
carbon nanotubes, new con
developments in nanotechn
tion of explosives. The mo
for the detection of hazard
Josephson junctions, NMR
Participants benefitted fro
CBRN agents using chem
problems of the physics of
cles, identification of partic
nanoparticles.

We are grateful to m
A. Balatsky and D. Logan f

Chapter 1
Spin Control in Quantum Dots for Quantum Information Processing

S. Prabhakar, R. Melnik, and L.L. Bonilla

Abstract In this paper, a detailed analysis of anisotropic effects on the phonon induced spin relaxation rate in InAs semiconductor quantum dots (QDs) is carried out for possible implementation towards QDs in security devices, encrypted data and quantum information processing. We show that anisotropic gate potentials enhance the phonon mediated spin-flip rate and reduce the cusp-like structure to lower magnetic fields.

1.1 Introduction

A critical ingredient for the design of robust spintronic devices for the feasibility of the quantum information processing is the accurate estimation of the spin relaxation rate. Usually the spin relaxation time or decohenrence time is supposed to be larger than for the gate operation time for the possible implementation of quantum dots in security devices, encrypted data and quantum information processing. Recent studies by authors in Refs. [7, 11] have measured long spin relaxation times of 0.85 ms in GaAs QDs by pulsed relaxation rate measurements and 20 ms in InGaAs QDs by optical orientation measurements. These experimental studies in QDs confirm that the manipulation of spin-flip rate by spin-orbit coupling with respect to the environment is important for the design of robust spintronics logic devices [8, 9, 16]. The spin-orbit coupling is mainly dominated by the Rashba [3] and the linear Dresselhaus [6] terms in solid state QDs. The Rashba spin-orbit coupling arises from structural inversion asymmetry along the growth direction and

S. Prabhakar (✉) • R. Melnik
M^2NeT Laboratory, Wilfrid Laurier University, Waterloo, ON, N2L 3C5 Canada
e-mail: sprabhakar@wlu.ca

L.L. Bonilla
Gregorio Millan Institute, Universidad Carlos III de Madrid, 28911, Leganes, Spain

J. Bonča and S. Kruchinin (eds.), *Nanotechnology in the Security Systems*,
NATO Science for Peace and Security Series C: Environmental Security,
DOI 10.1007/978-94-017-9005-5_1, © Springer Science+Business Media Dordrecht 2015

the Dresselhaus spin-orbit coupling arises from the bulk inversion asymmetry of the crystal lattice [1, 2, 22]. Recently, electric and magnetic fields tunability of the electron spin states in gated III–V semiconductor QDs was manipulated through Rashba and Dresselhaus spin-orbit couplings [13, 15, 20–22].

Anisotropic effects, induced in the orbital angular momentum in QDs, suppress the Landé g-factor towards the bulk crystal [15, 17]. g-factor can be manipulated through strong Rashba spin-orbit coupling in InAs QDs [17] and through strong Dresselhaus spin-orbit coupling in GaAs QDs [15]. Large anisotropy effects of the spin-orbit interaction in self-assembled InAs QDs have recently been studied experimentally in Ref. [25]. In this paper, we study the phonon induced spin-flip rate of electron spin states in both isotropic and anisotropic QDs at absolute zero temperature. Our studies show that the Rashba spin-orbit coupling has an appreciable contribution to the spin-flip rate in InAs QDs. However, the Rashba spin-orbit coupling has a contribution to the spin-flip rate in GaAs QDs near the level crossing point and the Dresselhaus spin-orbit coupling elsewhere. Anisotropic gate potentials, playing an important role in the spin-flip rate, can be used to manipulate the accidental degeneracy due to level crossing between the electron spin states $|0,0,-\rangle$ and $|0,1,+\rangle$. Here we label the Fock–Darwin states as $|n_+, n_-, \pm\rangle$ (see Eq. (1.3)) with $\pm$ being the eigenstates of the Pauli spin matrix [15, 19, 22]. In this paper, we show that the anisotropic gate potentials cause also a quenching effect in the orbital angular momentum that enhances the phonon mediated spin-flip rate and reduces its cusp-like structure to lower magnetic fields, in addition to lower QDs radii.

1.2 Theoretical Model

We consider 2D anisotropic III-V semiconductor QDs in the presence of a magnetic field along the growth direction. The total Hamiltonian of an electron in anisotropic QDs including spin-orbit interaction can be written as [2, 9, 22]

$$H = H_{xy} + H_z + H_{so}, \tag{1.1}$$

where the Hamiltonian H_{so} is associated with the Rashba–Dresselhaus spin-orbit couplings, H_z is the Hamiltonian of an electron along the growth z-direction and H_{xy} is the Hamiltonian of the electron in anisotropic QDs. H_{xy} can be written as

$$H_{xy} = \frac{\boldsymbol{P}^2}{2m} + \frac{1}{2}m\omega_o^2(ax^2 + by^2) + \frac{1}{2}g_o\mu_B\sigma_z B, \tag{1.2}$$

where $\boldsymbol{P} = \boldsymbol{p} + e\boldsymbol{A}$ is the kinetic momentum operator, $\boldsymbol{p} = -i\hbar(\partial_x, \partial_y, 0)$ is the canonical momentum operator, $\boldsymbol{A}$ is the vector potential in the asymmetric gauge, m is the effective mass of the electron in the conduction band, μ_B is the

Bohr magneton, $\boldsymbol{\sigma} = (\sigma_x, \sigma_y, \sigma_z)$ are the Pauli spin matrices, $\omega_0 = \hbar/m\ell_0^2$ is the parabolic confining potential and ℓ_0 is the radius of the QDs.

The above Hamiltonian represents the superposition of two independent harmonic oscillators. The energy spectrum of H_{xy} can be written as

$$\varepsilon_{n_+ n_-} = (n_+ + n_- + 1)\,\hbar\omega_+ + (n_+ - n_-)\,\hbar\omega_- + \frac{1}{2} g_0 \mu_B \sigma_z B, \tag{1.3}$$

where $n_\pm$ are the eigenvalues of the number operators $a^\dagger_\pm a_\pm$. Here, $a_\pm$ and $a^\dagger_\pm$ are usual annihilation ("lowering") and creation ("raising") operators. In Eq. (1.3), we included Zeeman spin splitting energy and

$$\omega_\pm = \frac{1}{2}\left[\omega_c^2 + \omega_0^2\left(\sqrt{a} \pm \sqrt{b}\right)^2\right]^{1/2}. \tag{1.4}$$

The second term in (1.1) represents the Hamiltonian of the electron along z-direction i.e., $H_z = p_z^2/2m + V(z)$, where V_z is the asymmetric triangular quantum well confining potential along z-direction. Usually, the asymmetric triangular quantum well potential can be found by solving Schrödinger–Poisson equation self-consistently [12, 15, 24]. The potential along z-direction can be chosen as $V_z = eEz$ for $z \geq 0$ and $V_z = \infty$ for $z\langle 0$ [22]. The ground state wavefunction ($\Psi_{0z}(z)$) of H_z can be written in the form of Airy function (Ai) as [15, 22, 24]

$$\Psi_{0z}(z) = 1.4261 k^{1/2} Ai\,(kz + \varphi_1), \tag{1.5}$$

where $\varphi_1 = -2.3381$ is the first zero of the Airy function and

$$k = \left[\frac{2meE}{\hbar^2}\right]^{1/3}. \tag{1.6}$$

Since $\left[H_{xy}, H_z\right] = 0$, we use the momentum along z-direction as a good quantum number i.e., $\langle p_z^2\rangle = 0.78\,(\hbar k)^2$ and $\langle z\rangle = 1.56/k$ estimates the thickness of the two dimensional electron gas (2DEG).

Finally, the Hamiltonian associated with the Rashba and linear Dresselhaus spin-orbit couplings can be written as [3, 6, 22]

$$H_{so} = \frac{\alpha_R}{\hbar}\left(\sigma_x P_y - \sigma_y P_x\right) + \frac{\alpha_D}{\hbar}\left(-\sigma_x P_x + \sigma_y P_y\right), \tag{1.7}$$

where the strengths of the Rashba and Dresselhaus spin-orbit couplings are characterized by the parameters α_R and α_D. They are given by

$$\alpha_R = \gamma_R e E, \quad \alpha_D = 0.78\gamma_D\left(\frac{2me}{\hbar^2}\right)^{2/3} E^{2/3}, \tag{1.8}$$

where γ_R and γ_D are the Rashba and Dresselhaus coefficients.

The Hamiltonian (1.7) can be written in terms of raising and lowering operators as

$$
\begin{aligned}
H_{so} = {} & \alpha_R (1+i)\,[b^{1/4}\kappa_+ (s_+ - i)\, a_+ + b^{1/4}\kappa_+ (s_- + i)\, a_- \\
& + a^{1/4}\eta_- (i - s_-)\, a_+ + a^{1/4}\eta_- (i + s_+)\, a_-] \\
& + \alpha_D (1+i)\,[a^{1/4}\kappa_- (i - s_-)\, a_+ + a^{1/4}\kappa_- (i + s_+)\, a_- \\
& + b^{1/4}\eta_+ (-i + s_+)\, a_+ + b^{1/4}\eta_+ (i + s_-)\, a_-] + H.c.,
\end{aligned}
\tag{1.9}
$$

where

$$
\kappa_\pm = \frac{1}{2\,(s_+ - s_-)} \left\{ \frac{1}{\ell}\sigma_x \pm i \frac{eB\ell}{\hbar} \left(\frac{1}{\sqrt{a} + \sqrt{b}} \right) \sigma_y \right\}, \tag{1.10}
$$

$$
\eta_\pm = \frac{1}{2\,(s_+ - s_-)} \left\{ \frac{1}{\ell}\sigma_y \pm i \frac{eB\ell}{\hbar} \left(\frac{1}{\sqrt{a} + \sqrt{b}} \right) \sigma_x \right\}, \tag{1.11}
$$

$$
s_\pm = \frac{\omega_+}{\omega_c \left(\frac{b}{a}\right)^{\frac{1}{4}}} \left[\sqrt{\frac{b}{a}} - 1 \pm \left[\frac{\omega_c^2 \sqrt{\frac{b}{a}}}{\omega_+^2} + \left(1 - \sqrt{\frac{b}{a}} \right)^2 \right]^{\frac{1}{2}} \right]. \tag{1.12}
$$

H.c. represents the Hermitian conjugate, $\ell = \sqrt{\hbar/m\Omega}$ is the hybrid orbital length and $\Omega = \sqrt{\omega_0^2 + \omega_c^2/4}$. It is clear that the spin-orbit Hamiltonian and the Zeeman spin splitting energy in both isotropic and anisotropic QDs obey a selection rule in which the orbital angular momentum can change by one quantum.

At low electric fields and small QDs radii, we treat the Hamiltonian associated with the Rashba and linear Dresselhaus spin-orbit couplings as a perturbation. Using second order perturbation theory, the energy spectrum of the electron spin states in QDs is given by

$$
\varepsilon_{0,0,+} = \hbar\varpi_+ - \frac{\alpha_R^2 \xi_+ + \alpha_D^2 \varsigma_+}{\hbar\omega_x - \Delta} - \frac{\alpha_R^2 \varsigma_- + \alpha_D^2 \xi_-}{\hbar\omega_y - \Delta}, \tag{1.13}
$$

$$
\varepsilon_{0,0,-} = \hbar\varpi_- - \frac{\alpha_R^2 \varsigma_+ + \alpha_D^2 \xi_+}{\hbar\omega_x + \Delta} - \frac{\alpha_R^2 \xi_- + \alpha_D^2 \varsigma_-}{\hbar\omega_y + \Delta}, \tag{1.14}
$$

where $\varpi_\pm = \omega_+ \pm \omega_z/2$, $\omega_z = \Delta/\hbar$ is the Zeeman frequency, $\Delta = g_0\mu_B B$, $\omega_x = \omega_+ + \omega_-$, and $\omega_y = \omega_+ - \omega_-$. Also,

$$
\xi_\pm = \frac{1}{2(s_+ - s_-)} \left\{ \pm \frac{1}{s_\pm}\alpha_\pm^2 + 2\alpha_\pm\beta_\pm \mp \frac{1}{s_\mp}\beta_\pm^2 \right\}. \tag{1.15}
$$

$$\varsigma_{\pm} = \frac{1}{2(s_{+} - s_{-})}\left\{\pm\frac{1}{s_{\pm}}\alpha_{\mp}^{2} - 2\alpha_{\mp}\beta_{\mp} \mp \frac{1}{s_{\mp}}\beta_{\mp}^{2}\right\}, \tag{1.16}$$

$$\alpha_{\pm} = a^{1/4}\left\{\frac{1}{\ell} \pm \frac{eB\ell}{\hbar}\frac{1}{\left(\sqrt{a}+\sqrt{b}\right)}\right\}, \tag{1.17}$$

$$\beta_{\pm} = b^{1/4}\left\{\frac{1}{\ell} \pm \frac{eB\ell}{\hbar}\frac{1}{\left(\sqrt{a}+\sqrt{b}\right)}\right\}. \tag{1.18}$$

We now turn to the calculation of the phonon induced spin relaxation rate at absolute zero temperature between two lowest energy states in QDs. Following Ref. [18], the interaction between electron and piezo-phonon can be written as [9, 10, 14, 26]

$$u_{ph}^{\mathbf{q}\alpha}(\mathbf{r},t) = \sqrt{\frac{\hbar}{2\rho V\omega_{\mathbf{q}\alpha}}}e^{i(\mathbf{q}\cdot\mathbf{r}-\omega_{q\alpha}t)}eA_{\mathbf{q}\alpha}b_{\mathbf{q}\alpha}^{\dagger} + H.c. \tag{1.19}$$

Here, ρ is the crystal mass density, V is the volume of the QDs, $b_{\mathbf{q}\alpha}^{\dagger}$ creates an acoustic phonon with wave vector $\mathbf{q}$ and polarization $\hat{e}_{\alpha}$, where $\alpha = l, t_1, t_2$ are chosen as one longitudinal and two transverse modes of the induced phonon in the dots. Also, $A_{\mathbf{q}\alpha} = \hat{q}_i\hat{q}_k e\beta_{ijk}e_{\mathbf{q}\alpha}^{j}$ is the amplitude of the electric field created by phonon strain, where $\hat{\mathbf{q}} = \mathbf{q}/q$ and $e\beta_{ijk} = eh_{14}$ for $i \neq k, i \neq j, j \neq k$. The polarization directions of the induced phonon are $\hat{e}_l = (\sin\theta\cos\phi, \sin\theta\sin\phi, \cos\theta)$, $\hat{e}_{t_1} = (\cos\theta\cos\phi, \cos\theta\sin\phi, -\sin\theta)$ and $\hat{e}_{t_2} = (-\sin\phi, \cos\phi, 0)$. Based on the Fermi Golden Rule, the phonon induced spin transition rate in the QDs is given by [10, 22]

$$\frac{1}{T_1} = \frac{2\pi}{\hbar}\int\frac{d^3\mathbf{q}}{(2\pi)^3}\sum_{\alpha=l,t}|M(\mathbf{q}\alpha)|^2\delta(\hbar s_{\alpha}\mathbf{q} - \varepsilon_{0,0,-} + \varepsilon_{0,0,+}), \tag{1.20}$$

where s_l, s_t are the longitudinal and transverse acoustic phonon velocities in QDs. The matrix element $M(\mathbf{q}\alpha)$ for the spin-flip rate between the Zeeman sublevels with the emission of phonon $\mathbf{q}\alpha$ has been calculated perturbatively [10, 23]. As a result, we have:

$$\frac{1}{T_1} = c\left(|M_x|^2 + |M_y|^2\right), \tag{1.21}$$

where

$$c = \frac{2(eh_{14})^2(g\mu_B B)^3}{35\pi\hbar^4\rho}\left(\frac{1}{s_l^5} + \frac{4}{3}\frac{1}{s_t^5}\right), \tag{1.22}$$

$$M_x = \frac{(is_- + 1)\,\Xi_1\,(\hbar\omega_x + \Delta) + (-is_- + 1)\,\Xi_3\,(\hbar\omega_x - \Delta)}{a^{1/4}\left[(\hbar\omega_x)^2 - \Delta^2\right]}$$
$$+ \frac{(-is_+ + 1)\,\Xi_2\,(\hbar\omega_y + \Delta) + (is_+ + 1)\,\Xi_4\,(\hbar\omega_y - \Delta)}{a^{1/4}\left[(\hbar\omega_y)^2 - \Delta^2\right]}. \tag{1.23}$$

$$M_y = \frac{(is_+ + 1)\,\Xi_1\,(\hbar\omega_x + \Delta) + (-is_+ + 1)\,\Xi_3\,(\hbar\omega_x - \Delta)}{b^{1/4}\left[(\hbar\omega_x)^2 - \Delta^2\right]}$$
$$+ \frac{(is_- - 1)\,\Xi_2\,(\hbar\omega_y + \Delta) + (-is_- - 1)\,\Xi_4\,(\hbar\omega_y - \Delta)}{b^{1/4}\left[(\hbar\omega_y)^2 - \Delta^2\right]}. \tag{1.24}$$

$$\Xi_1 = \ell'[\alpha_R\,\{(s_+ + i)\,\beta_+ + (1 - is_-)\,\alpha_+\}$$
$$+\alpha_D\,\{(-s_- - i)\,\alpha_- + (-1 + is_+)\,\beta_-\}]. \tag{1.25}$$
$$\Xi_2 = \ell'[\alpha_R\,\{(s_- - i)\,\beta_+ + (1 + is_+)\,\alpha_+\}$$
$$+\alpha_D\,\{(s_+ - i)\,\alpha_- + (1 + is_-)\,\beta_-\}]. \tag{1.26}$$
$$\Xi_3 = \ell'[\alpha_R\,\{(s_+ - i)\,\beta_- + (-1 - is_-)\,\alpha_-\}$$
$$+\alpha_D\,\{(-s_- + i)\,\alpha_+ + (1 + is_+)\,\beta_+\}]. \tag{1.27}$$
$$\Xi_4 = \ell'[\alpha_R\,\{(s_- + i)\,\beta_- + (-1 + is_+)\,\alpha_-\}$$
$$+\alpha_D\,\{(s_+ + i)\,\alpha_+ + (-1 + is_-)\,\beta_+\}]. \tag{1.28}$$

where $\ell' = \ell/\left(2\,(s_+ - s_-)^2\right)$. In the above expression, we use $c = c_l I_{xl} + 2c_t I_{xt}$, where $c_\alpha = \frac{q^2e^2}{(2\pi)^2\hbar^2 s_\alpha}|\varepsilon_{q\alpha}|^2$, $|\varepsilon_{q\alpha}|^2 = \frac{q^2\hbar}{2\rho\omega_{q\alpha}}$ and $q = \frac{g\mu_B B}{\hbar s_\alpha}$. Also, $g = \frac{\varepsilon_{0,0,-} - \varepsilon_{0,0,+}}{\mu_B B}$ is the Landé g-factor. For longitudinal phonon modes, [8, 10] we have $|A_{q,l}|^2 = 36h_{14}^2\cos^2\theta\sin^4\theta\sin^2\phi\cos^2\phi$ and

$$I_{xl} = \int_{\theta=0}^{\pi}\int_{\phi=0}^{2\pi} d\theta d\phi\,\sin^3\theta\cos^2\phi|A_{ql}|^2 = \frac{16\pi}{35}h_{14}^2, \tag{1.29}$$

$$I_{yl} = \int_{\theta=0}^{\pi}\int_{\phi=0}^{2\pi} d\theta d\phi\,\sin^3\theta\sin^2\phi|A_{ql}|^2 = \frac{16\pi}{35}h_{14}^2, \tag{1.30}$$

$$I_{xyl} = \int_{\theta=0}^{\pi}\int_{\phi=0}^{2\pi} d\theta d\phi\,\sin^3\theta\sin 2\phi|A_{ql}|^2 = 0. \tag{1.31}$$

For transverse phonon modes, [8, 10]
$|A_{q,t}|^2 = 2h_{14}^2[\cos^2\theta\sin^2\theta + \sin^4\theta\left(1 - 9\cos^2\theta\right)\sin^2\phi\cos^2\phi]$ and

$$I_{xt} = \int_{\theta=0}^{\pi} \int_{\phi=0}^{2\pi} d\theta d\phi \sin^3\theta \cos^2\phi |A_{qt}|^2 = \frac{32\pi}{105} h_{14}^2. \tag{1.32}$$

$$I_{yt} = \int_{\theta=0}^{\pi} \int_{\phi=0}^{2\pi} d\theta d\phi \sin^3\theta \sin^2\phi |A_{qt}|^2 = \frac{32\pi}{105} h_{14}^2. \tag{1.33}$$

$$I_{xyt} = \int_{\theta=0}^{\pi} \int_{\phi=0}^{2\pi} d\theta d\phi \sin^3\theta \sin 2\phi |A_{qt}|^2 = 0. \tag{1.34}$$

For isotropic QDs ($a = b = 1, s_+ = 1$ and $s_- = -1$), the spin relaxation rate is given by

$$\frac{1}{T_1} = \frac{2\,(eh_{14})^2\,(g\mu_B B)^3}{35\pi\hbar^4\rho} \left(\frac{1}{s_l^5} + \frac{4}{3}\frac{1}{s_t^5}\right) \left(|M_R|^2 + |M_D|^2\right), \tag{1.35}$$

where M_R and M_D are the coefficients of matrix element associated with the Rashba and Dresselhaus spin-orbit couplings in QDs and are given by

$$M_R = \frac{\alpha_R}{\sqrt{2}\hbar\Omega} \left[\frac{1}{1 - \frac{\Delta}{\hbar(\Omega + \frac{\omega_c}{2})}} - \frac{1}{1 + \frac{\Delta}{\hbar(\Omega - \frac{\omega_c}{2})}} \right], \tag{1.36}$$

$$M_D = \frac{\alpha_D}{\sqrt{2}\hbar\Omega} \left[\frac{1}{1 + \frac{\Delta}{\hbar(\Omega + \frac{\omega_c}{2})}} - \frac{1}{1 - \frac{\Delta}{\hbar(\Omega - \frac{\omega_c}{2})}} \right]. \tag{1.37}$$

Since $\Delta = g_0\mu_B B$ is negative for GaAs and InAs QDs, it means that the degeneracy only appears in the Rashba case (see 2nd term of Eq. (1.36)) and is absent in the Dresselhaus case. Similarly, the degeneracy only appears in the g-factor for the Rashba spin-orbit coupling [17]. The degeneracy in the Rashba case induces the level crossing point and cusp-like structure in the spin-flip rate in QDs. By considering second power of Δ, the spin relaxation rate for isotropic QDs is given by

$$\frac{1}{T_1} = \frac{2\,(eh_{14})^2\,(g\mu_B B)^3}{35\pi\hbar^4\rho} \left(\frac{1}{s_l^5} + \frac{4}{3}\frac{1}{s_t^5}\right) \frac{2\Delta^2}{\hbar^4\Omega^4} \left(\alpha_R^2 + \alpha_D^2\right)$$
$$\left[1 + 2\left(\frac{\omega_c}{2\Omega}\right)^2 + 3\left(\frac{\omega_c}{2\Omega}\right)^4 + \cdots\right]. \tag{1.38}$$

It can be seen that the spin-flip rate is highly sensitive to the effective g-factor of the electron, Zeeman energy, hybrid orbital frequency and cyclotron frequency of the QDs.

1.3 Results and Discussions

In Fig. 1.1, we investigate the contributions of the Rashba and the Dresselhaus spin-orbit couplings on the phonon induced spin relaxation rate as a function of magnetic fields in symmetric InAs QDs. Since the strength of the Dresselhaus spin-orbit coupling is much smaller than the Rashba spin-orbit coupling ($\frac{\alpha_R}{\alpha_D} = 3.2$ at $E = 10^5$ V/cm (see Eq. (1.8))), only the Rashba spin-orbit coupling has a major contribution to the phonon induced spin-flip rate. The cusp-like structure is absent (see Fig. 1.1 (dashed line)) and the spin-flip rate $(1/T_1)$ is a monotonic function of magnetic field (B) for the pure Dresselhaus case $(\alpha_R = 0)$. We solve the corresponding eigenvalue problem with Hamiltonian (1.1) by applying the exact diagonalization procedure and the Finite Element Method, [5, 15] obtaining the energy levels. The inset plots show the energy difference vs. magnetic field (Fig. 1.1(i)) and effective Landé g-factor vs. magnetic field (Fig. 1.1(ii)). It can be seen that the level crossing point occurs at $B = 3.5T$ which is the exact location of the accidental degeneracy point in the spin-flip rate either for the pure Rashba case $(\alpha_D = 0)$ or the mixed case (both α_R and α_D are present). Similar results have been discussed in Refs. [1, 2] and we consider these results as a benchmark for further investigation of anisotropic orbital effects on the spin-flip rate in QDs.

Figure 1.2 explores the influence of anisotropic effects on the spin-flip rate vs. magnetic fields for the electric fields $E = 10^4, 5 \times 10^4, 10^5$ V/cm. It can be seen that

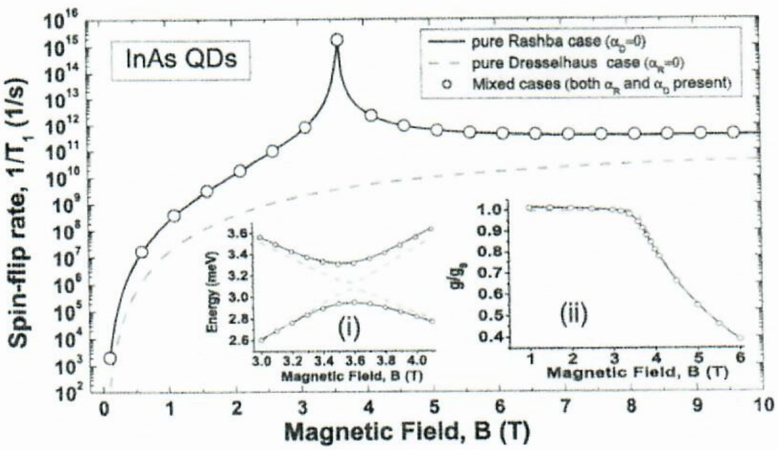

Fig. 1.1 (Color online) Contributions of Rashba and Dresselhaus spin-orbit couplings on the phonon induced spin-flip rate vs magnetic fields in InAs QDs. Inset plots show the energy difference vs. magnetic fields near the level crossing point and the g-factor vs magnetic fields. Here we choose $E = 10^5$ V/cm, $\ell_0 = 20$ nm and $a = b = 1$. The material constants for InAs QDs are chosen from Refs. [4, 22] as $g_0 = -15$, $m = 0.0239$, $\gamma_R = 110\,\text{Å}^2$, $\gamma_D = 130\,\text{eVÅ}^3$, $eh_{14} = 0.54 \times 10^{-5}$ erg/cm, $s_l = 4.2 \times 10^5$ cm/s, $s_t = 2.35 \times 10^5$ cm/s and $\rho = 5.6670$ g/cm^3

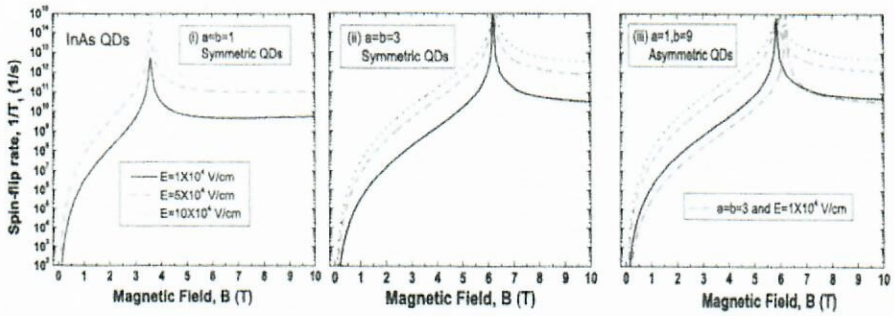

Fig. 1.2 (Color online) Spin relaxation rate ($1/T_1$) vs magnetic fields between the states $|0, 0, +\rangle$ and $|0, 0, -\rangle$ in InAs QDs. Here we chose $\ell_0 = 20\,\text{nm}$ (the QD radius). As a reference in Fig. 1.2(iii), *dashed-dotted line* represents the spin-flip rate for symmetric QDs with $a = b = 3$. We see that the anisotropic potential enhances the spin-flip rate and reduces the level crossing point to lower magnetic fields

the enhancement in the spin-flip rate occurs with the increase in electric fields. The accidental degeneracy point in the spin-flip rate is not affected by the electric fields which tells us that it is purely an orbital effect and is independent of the Rashba–Dresselhaus spin-orbit interaction. In Fig. 1.2(ii), the accidental degeneracy point is found at the magnetic field $B = 3.5T$. However, this point increases to the larger magnetic field $B = 6.2T$ in Fig. 1.2(ii). The extension in the B-field tunability of the spin-flip rate mainly occurs due to an increase in the area of the symmetric quantum dots. Note that the area of the quantum dots in Fig. 1.2(ii) is nine times larger than of the dots in Fig. 1.2(i). We quantify the influence of anisotropic effects on the spin-flip rate in Fig. 1.2(iii). Here we find that the quenching in the orbital angular momentum [20, 21] enhances the spin-flip rate and reduces the accidental degeneracy point to lower magnetic fields ($B = 5.85T$) compared to the symmetric quantum dots ($B = 6.2T$). As a reference, in Fig. 1.2(iii), we also plotted the spin-flip rate vs. magnetic fields (shown by dashed-dotted line) for symmetric QDs ($a = b = 3$) at $E = 10^4\,\text{V/cm}$ and $\ell_0 = 20\,\text{nm}$. Note that the area of the isotropic and anisotropic quantum dots in Fig. 1.2(ii) and (iii) are held constant. The expression for the level crossing point is given by the condition [1,2] $\varepsilon^0_{0,0,-} = \varepsilon^0_{0,1,+}$ i.e., $\hbar\,(\omega_+ - \omega_-) = |g_0|\mu_B B$ (see Eq. (1.3)). For isotropic QDs ($a = b = 1$), the condition for the level crossing point is $\Omega - \omega_c/2 = |g_0|\mu_B B/\hbar$. It means, when the difference between the hybrid orbital frequency to the half of the cyclotron frequency becomes equal to the Zeeman frequency then the degeneracy appears in the energy spectrum which gives the level crossing point and cusp-like structure near the degeneracy in the spin-flip rate in QDs. If we compare the condition of the level crossing point for the isotropic and anisotropic QDs, we find that the anisotropic potential reduces the level crossing point to lower magnetic fields if the area of the symmetric and asymmetric quantum dots is held constant. However, if we increase the area, the level crossing point extends to a larger magnetic field.

1.4 Conclusions

In summary, we have analyzed in detail anisotropy effects on the electron spin relaxation rate in InAs QDs, using realistic parameters for possible implementation towards QDs in security devices, encrypted data and quantum information processing. In Fig. 1.1, we have shown that only the Rashba spin-orbit coupling has a major contribution on the phonon induced spin-flip rate. In Figs. 1.1 and 1.2, we have shown that a cusp-like structure due to the accidental degeneracy point appears in the phonon induced spin-flip rate and can be manipulated to lower magnetic fields with the application of anisotropic gate potentials. Also, we have shown that the anisotropic gate potential causes a quenching effect in the orbital angular momentum that enhances the phonon induced spin-flip rate.

Acknowledgements This work has been supported by NSERC and CRC programs (Canada).

References

1. Bulaev DV, Loss D (2005) Spin relaxation and anticrossing in quantum dots: Rashba versus dresselhaus spin-orbit coupling. Phys Rev B 71:205324
2. Bulaev DV, Loss D (2005) Spin relaxation and decoherence of holes in quantum dots. Phys Rev Lett 95:076805
3. Bychkov YA, Rashba EI (1984) Oscillatory effects and the magnetic susceptibility of carriers in inversion layers. J Phys C Solid State Phys 17:6039
4. Cardona M, Christensen NE, Fasol G (1988) Relativistic band structure and spin-orbit splitting of zinc-blende-type semiconductors. Phys Rev B 38:1806
5. Comsol multiphysics version 3.5a. (www.comsol.com).
6. Dresselhaus G (1955) Spin-orbit coupling effects in zinc blende structures. Phys Rev 100:580
7. Elzerman JM, Hanson R,Willems van Beveren LH,Witkamp B, Vandersypen LMK, Kouwenhoven LP (2004) Single-shot read-out of an individual electron spin in a quantum dot. Nature 430:431
8. Golovach VN, Khaetskii A, Loss D (2004) Phonon-induced decay of the electron spin in quantum dots. Phys Rev Lett 93:016601
9. Khaetskii AV, Nazarov YV (2000) Spin relaxation in semiconductor quantum dots. Phys Rev B 61:12639
10. Khaetskii AV, Nazarov YV (2001) Spin-flip transitions between zeeman sublevels in semiconductor quantum dots. Phys Rev B 64:125316
11. Kroutvar M, Ducommun Y, Heiss D, Bichler M, Schuh D, Abstreiter G, Finley JJ (2004) Optically programmable electron spin memory using semiconductor quantum dots. Nature 432:81
12. Mahapatra DR, Willatzen M, Melnik RVN, Lassen B (2012) Electron energy levels in GaAs-$Ga_{1-x}Al_xAs$ heterojunctions. NANO 07:1250031
13. Nowak MP, Szafran B, Peeters FM, Partoens B, Pasek WJ (2011) Tuning of the spin-orbit interaction in a quantum dot by an in-plane magnetic field. Phys Rev B 83:245324
14. Olendski O, Shahbazyan TV (2007) Theory of anisotropic spin relaxation in quantum dots. Phys Rev B 75:041306
15. Prabhakar S, Raynolds JE (2009) Gate control of a quantum dot single-electron spin in realistic confining potentials: Anisotropy effects. Phys Rev B 79:195307

16. Prabhakar S, Ra
a gaas quantum
technique. Phys
17. Prabhakar S, Ra
dots through the
and perturbation
18. Prabhakar S, Mc
phonon induced
19. Prabhakar S, M
relaxation rate in
Phys Rev B 87:2
20. Pryor CE, Flatté
tor quantum dot
21. Pryor CE, Flatté
semiconductor q
22. Sousa R, Sarma
Phys Rev B 68:1
23. Stano P, Fabian
Rev B 74:04532
24. Stern F, Sarma
Rev B 30:840
25. Takahashi S, De
(2010) Large an
dot. Phys Rev L
26. Woods LM, Re
B 66:161318

16. Prabhakar S, Raynolds J, Inomata A, Melnik R (2010) Manipulation of single electron spin in a gaas quantum dot through the application of geometric phases: The feynman disentangling technique. Phys Rev B 82:195306
17. Prabhakar S, Raynolds JE, Melnik R (2011) Manipulation of the landé g factor in inas quantum dots through the application of anisotropic gate potentials: Exact diagonalization, numerical, and perturbation methods. Phys Rev B 84:155208
18. Prabhakar S, Melnik R, Bonilla LL (2012) The influence of anisotropic gate potentials on the phonon induced spin-flip rate in gaas quantum dots. Appl Phys Lett 100:023108
19. Prabhakar S, Melnik R, Bonilla LL (2013) Electrical control of phonon-mediated spin relaxation rate in semiconductor quantum dots: Rashba versus dresselhaus spin-orbit coupling. Phys Rev B 87:235202
20. Pryor CE, Flatté ME (2006) Landé g factors and orbital momentum quenching in semiconductor quantum dots. Phys Rev Lett 96:026804
21. Pryor CE, Flatté ME (2007) Erratum: Landé g factors and orbital momentum quenching in semiconductor quantum dots. Phys Rev Lett 99:179901
22. Sousa R, Sarma S (2003) Gate control of spin dynamics in III-V semiconductor quantum dots. Phys Rev B 68:155330
23. Stano P, Fabian J (2006) Orbital and spin relaxation in single and coupled quantum dots. Phys Rev B 74:045320
24. Stern F, Sarma S (1984) Electron energy levels in GaAs-$Ga_{1-x}Al_xAs$ heterojunctions. Phys Rev B 30:840
25. Takahashi S, Deacon RS, Yoshida K, Oiwa A, Shibata K, Hirakawa K, Tokura Y, Tarucha S (2010) Large anisotropy of the spin-orbit interaction in a single InAs self-assembled quantum dot. Phys Rev Lett 104:246801
26. Woods LM, Reinecke TL, Lyanda-Geller Y (2002) Spin relaxation in quantum dots. Phys Rev B 66:161318

Contents

The topics discussed at the NATO Advanced Research Workshop "Nanotechnology in the Security Systems" included nanophysics, nanotechnology, nanomaterials, sensors, biosensors security systems, explosive detection. There have been many significant advances in the past two years and some entirely new directions of research are just opening up. Recent advances in nanoscience have demonstrated that fundamentally new physical phenomena are found when systems are reduced in size with dimensions, comparable to the fundamental microscopic length scales of the investigated material. Recent developments in nanotechnology and measurement techniques now allow experimental investigation of transport properties of nanodevices. This work will be of interest to researchers working in spintronics, molecular electronics and quantum information processing.

ISBN 978-94-017-9052-9

9 789401 790529

springer.com

ISBN 978-94-017-9052-9
ISSN 1874-6519